

KINEMATICS OF MOLECULAR CLOUDS. II. NEW DATA ON NEARBY GIANT MOLECULAR CLOUDS

ANTONY A. STARK
 AT&T Bell Laboratories

AND

JAN BRAND
 Max-Planck-Institut für Radioastronomie

Received 1988 January 11; accepted 1988 September 19

ABSTRACT

The best currently available data on positions, distances, and velocities of giant molecular clouds within 3 kpc of the Sun are analyzed to yield a one-dimensional rms cloud-to-cloud velocity dispersion $\sigma_v = 7.8_{-0.5}^{+0.6}$. Velocity dispersion is defined here as the root mean square of cloud peculiar velocities, a quantity which includes small-scale streaming. It is argued that this value for the velocity dispersion is plausible, based on examples of clouds whose velocities cannot be explained purely by galactic rotation. These anomalies are explained by the calculated value of σ_v , but substantially smaller values are unlikely. If streaming motions are not included in the dispersion, the value of σ_v is $\sim 20\%$ smaller. The mean motion of nearby molecular clouds is drifting by $\sim 4 \text{ km s}^{-1}$ with respect to the LSR.

Subject headings: galaxies: internal motions — interstellar: molecules — radial velocities

I. INTRODUCTION

The velocity dispersion of giant molecular clouds (GMCs) is important to some astrophysical theories. It appears in several places in galactic astronomy: in star formation, it governs the collision rate of molecular clouds; in galactic structure, it affects the stability of the galactic disk; in stellar dynamics, it affects the transfer of energy from interstellar clouds to random stellar motions. Because it is important to theory, evaluation of the velocity dispersion of GMCs is worth considerable observational effort and attention.

This paper is about the velocity dispersions of GMCs within a few kiloparsecs of the Sun. The approach taken is almost identical to that of § III in Paper I (Stark 1984); the method developed for that paper is here applied to a larger data base. In both of these papers, what is done is to consider the best available information on distances and velocities of GMCs which are associated with optically visible H II regions, and to reduce these data in such a way that the errors in the quantities and the uncertainties in the galactic rotation curve do not systematically bias the result. This paper evaluates the velocity dispersion of interstellar clouds within a few kiloparsecs of the Sun having masses typically 0.5 to $5 \times 10^5 M_\odot$. Various other approaches have been taken by observers to the more general problem of the velocity dispersion of molecular clouds of all masses throughout the Galaxy and in other galaxies. These will be discussed in § III.

Velocity dispersions can be defined in different ways. Different theoretical uses of the concept will use different definitions. Calculating a value for the quantity using real observational data requires a precise operational definition. The velocity dispersion is here defined to be the root-mean-square average of the peculiar velocities of an ensemble of galactic objects. The peculiar velocity of an object in the Galaxy is the difference between its actual velocity and the velocity it would have if it were moving with the purely circular, idealized velocity field of the galactic rotation. Additional issues are raised by this definition in the application of theory to observations, since the

circular velocity is a theoretical quantity which is not perfectly known in the real Galaxy.

Calculation of the peculiar velocity of an object also requires knowledge of its position, distance, and velocity. The observational error in these quantities propagate into the calculation of the peculiar velocities, but that error can be estimated, given the observational errors in the distance and velocity. Call the value of the peculiar velocity which has been calculated from observed quantities the *observed* peculiar velocity, to distinguish it from the *true* peculiar velocity, which is the actual value of the peculiar velocity, given perfect knowledge and perfect observations. The error in the observed peculiar velocity is particularly insidious, because the velocity dispersion is the rms average of the true peculiar velocities. The rms average of the *observed* peculiar velocities is greater than the rms average of the *true* peculiar velocities because the errors in the observed peculiar velocities make a positive contribution to the rms average. It is particularly easy to see that this is true in a hypothetical Galaxy where the true velocity dispersion of molecular clouds is identically zero, so that the true peculiar velocity of any given cloud is zero by definition. The observed peculiar velocity for the cloud would not be zero because of observational errors and because the velocity of a circular orbit is not precisely known, so the rms average of the peculiar velocities of an ensemble of clouds would be some positive number, overestimating the velocity dispersion of the clouds. The statistical method employed in this paper is designed to correct for this bias by removing the contribution of the observational errors from the calculation of the velocity dispersion, to the extent to which those errors are known. The calculation is not exact, but the problems are relegated to higher order.

The bias caused by observational uncertainty cannot be removed exactly if the observational errors are not known exactly: the uncertainty in the error can become a source of uncertainty in the velocity dispersion. This is potentially worrisome, because the observational uncertainties are very large in

some cases, and the values assigned to those uncertainties are little better than informed guesswork. This second-order problem will be treated by considering only a subset of the data that has small observational errors, and then arguing that if the errors themselves are small, then the uncertainty in the error estimates cannot be overly large.

II. CALCULATION OF THE VELOCITY DISPERSION

To begin we need a catalog of GMCs having known positions, velocities, and distances, along with errors in these quantities. At the time Paper I was written, the best available information about GMCs with optically visible H II regions had been summarized by Blitz, Fich, and Stark (1982, hereafter BFS). Now there are considerably more data, particularly data from southern observatories on objects in the third and fourth quadrants of the Galaxy. Most of these new data were collected by Brand, Blitz, and Wouterloot (1986, hereafter BBW) and Brand *et al.* (1987). The BFS and BBW catalogs were concatenated for the present paper, along with additional data from Chini and Wink (1984) and Forbes (1984). Many of the clouds in this catalog have distances with estimated errors; the remainder can be assigned a distance of 3.0 ± 3.5 kpc, since they are visually unobscured but are not in the immediate vicinity of the Sun.

For each cloud in the catalog, the expected radial velocity can be calculated:

$$v_{\text{rad}} = v_{\text{rad}}(l, b, r) = \left(\Theta \frac{R_{\odot}}{R} - \Theta_{\odot} \right) \sin l \cos b, \quad (1)$$

where the rotation curve is approximated by

$$\frac{\Theta}{\Theta_{\odot}} = 0.1121 \left(\frac{R}{R_{\odot}} \right)^{0.4142} + 0.90262 \quad (2)$$

(Brand 1986), $\Theta_{\odot} = 220 \text{ km s}^{-1}$ and $R_{\odot} = 8.5 \text{ kpc}$ and

$$R \equiv (R_{\odot}^2 + r^2 \cos^2 b - 2R_{\odot} r \cos b \cos l)^{1/2} \quad (3)$$

is the cloud's galactocentric distance. The error in this quantity can be estimated thus:

$$E(v_{\text{rad}}) \approx \frac{1}{2} |v_{\text{rad}}[l, b, r - E(r)] - v_{\text{rad}}[l, b, r + E(r)]| \quad (4)$$

[where $E(x)$ denotes the estimated error in x]. One definition of peculiar radial velocity is then

$$v_{\text{pec1}} \equiv v_{\text{LSR}} - v_{\text{rad}}, \quad (5)$$

where v_{LSR} is the observed radial velocity of the cloud, and

$$\epsilon \equiv E(v_{\text{pec1}}) \approx [E^2(v_{\text{LSR}}) + E^2(v_{\text{rad}})]^{1/2}. \quad (6)$$

The errors, ϵ , are the errors in the observed peculiar velocities. In the catalog values of ϵ range from 0.4 to 45 km s^{-1} .

This definition of peculiar velocity carries a potential problem. As in Paper I, there is a tendency to find positive values of v_{pec1} at large l and negative values at small l . This is shown in Figure 1. A χ^2 fit of $v = D_0 \cos(l - l_0) \cos b$ to the v_{pec1} yields $D_0 = 3.8 \pm 0.9 \text{ km s}^{-1}$ and $l_0 = 292 \pm 16^\circ$. The LSR as defined by disk stars is known with an error of $\sim 1 \text{ km s}^{-1}$ (Delhaye 1965). This fit therefore suggests a net drift between the stars and the GMCs. This drift should be

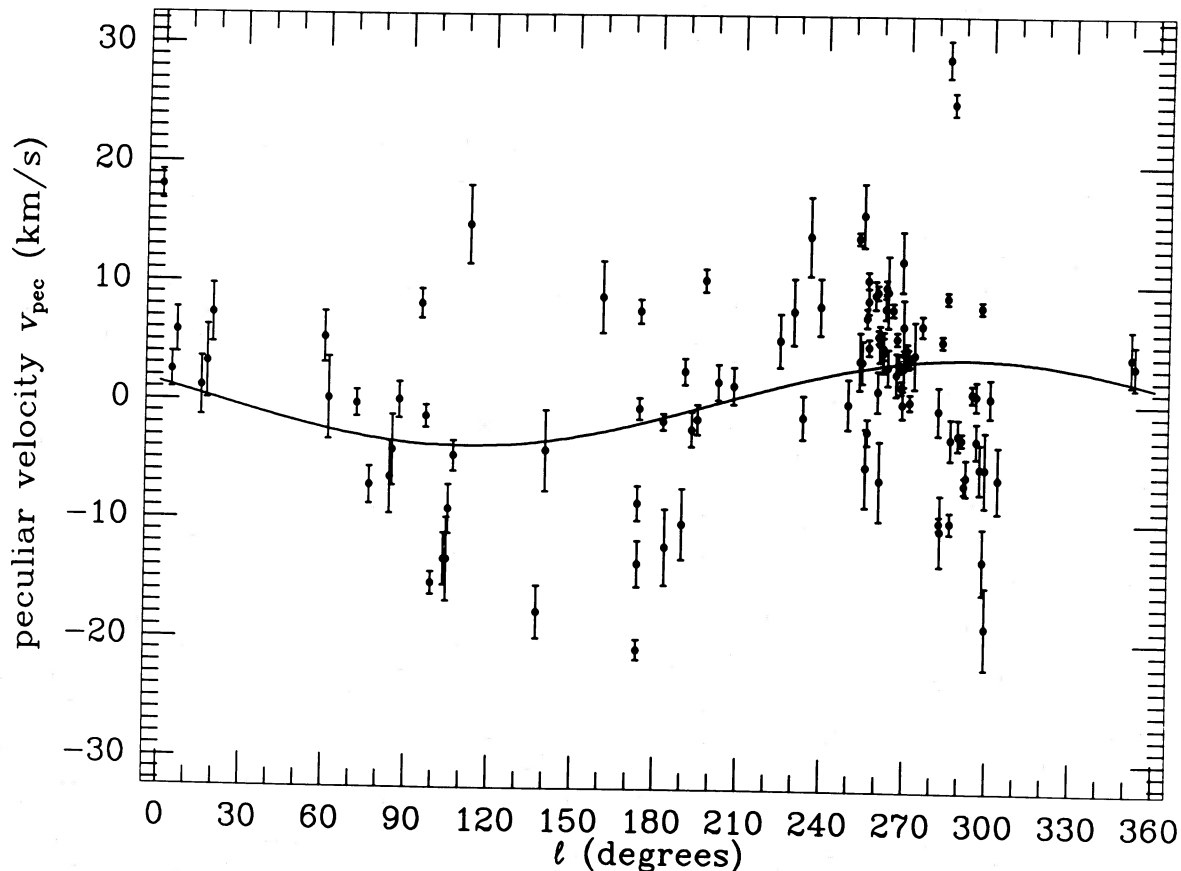


FIG. 1.—The peculiar radial velocities (v_{pec1}) from Table 1 plotted against l . The curve is the best fit function of the form $v = D_0 \cos(l - l_0) \cos b$. Error bars show $\pm 1 \sigma$ estimated errors.

TABLE 1
 NEARBY GMCs WITH ACCURATELY KNOWN PECULIAR RADIAL VELOCITIES
 (DISTANCE < 3 kpc AND $\epsilon_i < 3.5 \text{ km s}^{-1}$)

Cloud Name	LSR Velocity (km s ⁻¹)	<i>l</i>	<i>b</i>	Distance (kpc)	Peculiar Velocity 1 ^a (km s ⁻¹)	Peculiar Velocity 2 ^b (km s ⁻¹)
S16	18.10 ± 1.2	0.04	-0.39	3.00 ± 3.50	18.02 ± 1.22	16.60
S27	3.00 ± 1.5	4.24	22.51	0.17 ± 0.05	2.46 ± 1.50	1.39
S25	12.00 ± 1.7	5.95	-1.30	1.80 ± 0.20	5.80 ± 1.89	4.75
S45	20.00 ± 1.2	15.00	-0.68	2.20 ± 0.20	1.15 ± 2.45	0.68
S49	24.20 ± 2.0	17.06	0.70	2.20 ± 0.20	3.20 ± 3.09	2.87
S54	27.60 ± 0.5	18.90	2.09	2.00 ± 0.20	7.30 ± 2.46	7.09
S86	26.80 ± 1.4	59.66	-0.21	1.90 ± 0.20	5.36 ± 2.14	7.68
S87	22.80 ± 1.0	61.21	-0.05	2.20 ± 0.50	0.22 ± 3.46	2.62
S101	13.70 ± 0.4	71.59	2.76	2.50 ± 0.80	-0.21 ± 1.12	2.68
S106	-1.00 ± 1.5	76.40	-0.61	0.60 ± 0.10	-7.13 ± 1.56	-4.04
S112	-4.00 ± 2.0	83.78	3.28	2.10 ± 0.70	-6.44 ± 3.09	-3.10
S117	0.00 ± 3.0	84.68	-0.62	0.80 ± 0.30	-4.14 ± 3.00	-0.77
S119	3.50 ± 1.5	87.06	-4.19	0.70 ± 0.25	0.09 ± 1.51	3.52
S125	8.00 ± 1.0	94.72	-5.57	1.00 ± 0.16	8.19 ± 1.25	11.80
S126	-0.20 ± 0.4	96.72	-15.14	0.60 ± 0.20	-1.27 ± 0.95	2.27
S129	-13.90 ± 0.7	99.06	7.40	0.40 ± 0.13	-15.34 ± 0.95	-11.67
S134	-16.10 ± 0.5	103.70	2.18	0.88 ± 0.28	-13.33 ± 2.18	-9.57
S135	-20.70 ± 0.5	104.59	1.37	1.40 ± 0.40	-13.34 ± 3.49	-9.57
S137	-10.30 ± 1.4	105.15	7.12	0.62 ± 0.20	-9.13 ± 2.05	-5.39
S140	-8.50 ± 1.0	106.81	5.31	0.90 ± 0.10	-4.62 ± 1.31	-0.85
S161A	-10.00 ± 1.0	111.89	0.88	2.80 ± 0.30	14.86 ± 3.28	18.66
S199	-39.00 ± 1.0	137.30	1.40	2.10 ± 0.20	-17.73 ± 2.21	-14.30
S202	-11.50 ± 2.0	139.99	2.09	0.80 ± 0.25	-4.16 ± 3.44	-0.81
S220	7.00 ± 3.0	160.00	-19.00	0.40 ± 0.04	8.83 ± 3.01	11.23
S234	-13.40 ± 0.7	173.35	2.40	2.30 ± 0.70	-8.53 ± 1.45	-6.71
S232	-23.00 ± 0.5	173.43	3.17	1.00 ± 0.30	-20.82 ± 0.85	-19.00
S231	-18.40 ± 1.7	173.47	2.55	2.30 ± 0.50	-13.62 ± 1.92	-11.80
S238	7.60 ± 1.0	173.60	-1.78	0.15 ± 0.05	7.65 ± 1.01	9.45
S237	-4.30 ± 0.7	173.62	2.81	1.80 ± 0.30	-0.53 ± 0.90	1.27
S242	0.00 ± 0.5	182.36	0.19	2.10 ± 0.70	-1.61 ± 0.69	-0.33
BFS48	-9.10 ± 0.6	183.37	-0.56	3.00 ± 3.50	-12.19 ± 3.18	-10.97
S249	-5.30 ± 2.6	189.45	4.38	1.60 ± 0.50	-10.26 ± 2.98	-9.43
S252	7.50 ± 1.0	189.88	0.30	1.50 ± 0.15	2.62 ± 1.10	3.42
S254	7.50 ± 0.7	192.61	-0.04	2.50 ± 0.40	-2.25 ± 1.49	-1.63
S263	0.30 ± 1.0	194.59	-17.54	0.45 ± 0.14	-1.39 ± 1.25	-0.92
S264	12.00 ± 0.5	196.95	-10.29	0.40 ± 0.13	10.30 ± 0.96	10.63
S273	7.00 ± 1.0	202.00	1.60	0.80 ± 0.15	1.76 ± 1.50	1.76
S275	14.30 ± 0.1	207.50	-2.00	1.60 ± 0.20	1.46 ± 1.56	1.10
S292	16.70 ± 1.5	224.00	-2.00	1.15 ± 0.15	5.32 ± 2.25	3.90
BBW4	19.60 ± 0.5	228.97	-4.65	1.20 ± 0.24	7.74 ± 2.78	6.03
BBW41	16.70 ± 0.5	232.56	0.86	1.75 ± 0.16	-1.14 ± 1.84	-3.08
BBW42	43.00 ± 0.5	234.74	-0.27	2.81 ± 0.32	14.06 ± 3.32	12.01
BBW17B	20.60 ± 2.2	238.49	-4.66	1.35 ± 0.08	8.17 ± 2.38	5.92
BBW101	13.50 ± 0.5	248.90	-0.01	1.74 ± 0.20	-0.00 ± 2.10	-2.78
BBW104B	11.50 ± 0.5	252.39	-1.40	0.09 ± 0.02	13.93 ± 0.52	11.00
BBW106	10.90 ± 0.5	252.93	-1.90	1.27 ± 0.26	3.64 ± 2.41	0.69
BBW122	11.30 ± 0.5	253.81	-0.90	1.36 ± 0.19	3.58 ± 1.78	0.59
BBW124	35.10 ± 1.0	253.97	-0.39	2.58 ± 0.25	15.85 ± 2.67	12.85
BBW95	9.60 ± 0.5	255.52	-4.46	0.79 ± 0.08	7.26 ± 0.79	4.22
BBW109	5.10 ± 0.7	255.42	-3.04	1.75 ± 0.36	-5.34 ± 3.33	-8.39
BBW121	9.40 ± 0.5	255.68	-2.27	0.33 ± 0.07	10.43 ± 0.69	7.37
BBW56	-3.90 ± 1.1	255.83	-10.44	0.25 ± 0.02	-2.29 ± 1.11	-5.31
BBW119	9.80 ± 0.5	255.83	-2.60	0.64 ± 0.13	8.69 ± 1.07	5.62
BBW18	3.60 ± 0.5	256.14	-14.06	0.32 ± 0.07	4.82 ± 0.67	1.84
BBW143A	8.90 ± 1.0	258.31	-1.96	0.51 ± 0.10	9.22 ± 1.18	6.06
BBW129	9.40 ± 0.5	259.24	-3.66	0.59 ± 0.05	9.44 ± 0.58	6.25
BBW11	3.60 ± 0.5	259.56	-16.48	0.23 ± 0.05	5.74 ± 0.56	2.66
BBW141	10.00 ± 0.5	259.57	-2.82	1.85 ± 0.20	1.11 ± 1.72	-2.10
BBW160	7.10 ± 1.4	260.06	0.55	0.95 ± 0.09	5.13 ± 1.52	1.90
BBW93	3.00 ± 0.5	260.38	-7.99	2.00 ± 0.41	-6.46 ± 3.37	-9.67
BBW176	4.90 ± 0.8	261.38	0.84	0.72 ± 0.07	4.75 ± 0.89	1.48
BBW173	7.50 ± 0.5	261.47	0.32	1.21 ± 0.25	4.41 ± 1.72	1.14
BBW184	7.90 ± 0.5	262.09	1.17	0.70 ± 0.14	8.07 ± 0.89	4.77
BBW177	8.20 ± 0.5	262.18	0.36	0.40 ± 0.08	9.84 ± 0.61	6.54
BBW159	8.70 ± 3.0	262.86	-2.41	0.62 ± 0.03	9.48 ± 3.00	6.16
BBW192D	5.40 ± 0.5	263.11	1.61	1.20 ± 0.24	3.15 ± 1.52	-0.18
BBW206C	6.70 ± 0.5	264.70	1.45	0.61 ± 0.06	8.00 ± 0.55	4.62
BBW162	5.00 ± 0.5	266.07	-4.30	1.51 ± 0.31	2.55 ± 1.82	-0.86

TABLE 1—Continued

Cloud Name	LSR Velocity (km s ⁻¹)	<i>l</i>	<i>b</i>	Distance (kpc)	Peculiar Velocity 1 ^a (km s ⁻¹)	Peculiar Velocity 2 ^b (km s ⁻¹)
BBW137	3.10 ± 0.5	266.20	-7.79	0.36 ± 0.08	5.56 ± 0.54	2.17
BBW201	2.10 ± 0.5	266.98	-1.27	0.77 ± 0.16	3.47 ± 0.75	0.03
BBW237	-0.90 ± 0.5	267.95	1.81	0.52 ± 0.08	1.48 ± 0.54	-1.99
BBW195A	13.00 ± 2.3	268.16	-2.70	1.47 ± 0.21	12.01 ± 2.51	8.53
BBW193B	1.40 ± 0.8	268.45	-1.90	1.58 ± 0.17	0.04 ± 1.17	-3.44
BBW227	4.70 ± 2.2	268.59	-0.61	0.78 ± 0.16	6.57 ± 2.25	3.09
BBW235	0.80 ± 1.5	268.86	0.53	0.65 ± 0.13	3.10 ± 1.53	-0.40
BBW236	1.90 ± 0.5	270.02	-0.51	0.61 ± 0.12	4.60 ± 0.54	1.07
BBW239	2.10 ± 0.5	270.43	-0.27	1.07 ± 0.22	3.87 ± 0.81	0.33
BBW268	-2.60 ± 0.6	271.22	4.98	0.74 ± 0.15	0.23 ± 0.65	-3.31
BBW255	0.60 ± 0.5	271.23	0.96	0.53 ± 0.11	3.71 ± 0.51	0.16
BBW240	6.50 ± 0.5	272.83	-2.34	2.45 ± 0.50	4.16 ± 2.79	0.57
BBW265	3.20 ± 0.5	275.57	-2.20	1.57 ± 0.32	6.61 ± 0.86	2.97
BBW281	-7.00 ± 0.5	281.83	-2.07	2.63 ± 0.74	-0.50 ± 2.02	-4.24
BBW288	-18.00 ± 0.5	282.35	-1.39	1.97 ± 0.40	-9.94 ± 0.56	-13.69
BBW285	-17.60 ± 0.5	282.71	-2.48	2.82 ± 1.05	-10.60 ± 2.99	-14.34
BBW283	-3.10 ± 0.5	282.88	-3.14	1.64 ± 0.15	5.31 ± 0.51	1.57
BBW300B	19.30 ± 1.5	284.30	-0.31	2.31 ± 0.46	28.97 ± 1.54	25.20
BBW298	-1.20 ± 0.5	284.76	-3.06	2.21 ± 0.24	8.96 ± 0.51	5.19
BBW316D	-21.50 ± 0.9	286.21	-0.20	2.26 ± 0.16	-9.95 ± 0.90	-13.73
BBW309F	14.60 ± 0.5	286.28	-0.52	1.58 ± 0.32	25.22 ± 0.95	21.44
BBW321	-12.60 ± 0.5	286.35	3.24	1.26 ± 0.48	-2.91 ± 1.77	-6.69
BBW314	-13.60 ± 0.5	288.97	-3.84	1.28 ± 0.26	-2.52 ± 1.31	-6.31
BBW347	-19.20 ± 0.5	290.35	1.62	2.91 ± 0.34	-2.88 ± 0.54	-6.68
BBW348A	-24.00 ± 0.5	291.29	-0.68	2.65 ± 0.32	-6.78 ± 0.69	-10.58
BBW353	-23.00 ± 0.5	291.94	2.06	2.23 ± 0.45	-6.10 ± 1.51	-9.90
BBW362	-17.90 ± 0.5	294.04	-1.75	2.25 ± 0.13	0.96 ± 0.73	-2.83
BBW372	-13.40 ± 0.5	295.48	0.47	1.29 ± 0.15	0.77 ± 1.23	-3.02
BBW373	-16.20 ± 0.5	295.71	-0.34	1.15 ± 0.18	-3.01 ± 1.50	-6.80
BBW377	-29.80 ± 0.5	297.02	-1.71	2.90 ± 0.59	-5.39 ± 2.12	-9.18
BBW341	4.60 ± 0.5	297.25	-15.00	0.07 ± 0.01	8.17 ± 0.51	4.51
BBW382	-32.50 ± 0.5	298.42	0.69	1.78 ± 0.36	-13.15 ± 2.77	-16.93
BBW384	-25.70 ± 0.5	298.94	0.48	1.86 ± 0.41	-5.43 ± 3.16	-9.20
BBW387	-36.10 ± 2.2	299.46	-1.09	1.47 ± 0.30	-18.74 ± 3.42	-22.51
BBW396	-22.80 ± 0.5	300.53	-0.05	2.13 ± 0.20	0.58 ± 1.61	-3.18
BBW399	-23.30 ± 0.5	303.66	-3.51	1.28 ± 0.26	-6.28 ± 2.80	-9.99
S8	-4.30 ± 1.5	351.36	0.61	1.70 ± 0.31	4.02 ± 2.32	2.09
S11	-3.90 ± 1.0	352.80	0.64	1.74 ± 0.31	3.27 ± 1.81	1.42

^a Peculiar radial velocity has in this case been calculated assuming $\Theta_{\odot} = 220 \text{ km s}^{-1}$ and $R_{\odot} = 8.5 \text{ kpc}$, and the rotation curve described in § II. The error in this column is called ϵ_i in the text.

^b Residuals of the peculiar radial velocity 1 (v_{pec1}) to a χ^2 fit to $v_p = A \cos(l - l_0) \cos(b)$, where in this case $A = 3.8 \pm 0.9 \text{ km s}^{-1}$ and $l_0 = 292 \pm 16^\circ$.

removed, because we do not know whether the LSR or the velocity centroid of the GMCs is closer to the velocity of a circular orbit around the galactic center. Leaving in the contribution of this drift would bias upward the estimate of the velocity dispersion. A second definition of the peculiar velocities is then

$$v_{\text{pec2}} \equiv v_{\text{pec1}} - D_0 \cos(l - l_0) \cos b. \quad (7)$$

Imagine a series of subsets of the BFs and BBW catalogs, each described by a different maximum allowed error ϵ_{max} , so that $\epsilon \leq \epsilon_{\text{max}}$ for all members of that subset. Table 1 is such a subset for $\epsilon_{\text{max}} = 3.5 \text{ km s}^{-1}$. As ϵ_{max} increases, more and more clouds are allowed into consideration, but the new data are of declining quality. As ϵ_{max} becomes large, the error in the ϵ values will also become large, and at some level this "error in the error" will begin to contaminate the result. Since the "error in the error" will contribute in quadrature, and since it is likely to be the same size or smaller than the ϵ values themselves, we obviate this problem by restricting ϵ_{max} to values less than, say, half of the velocity dispersion. At this point we do not know the result (the velocity dispersion) so we allow all of

the various subsets of the data. Consider a particular but as yet unspecified value of ϵ_{max} , so that we have a single subset of the catalog where each member has a different subscript, i . To remove the LSR drift, a χ^2 fit is performed on the subset to determine l_0 and D_0 for this ensemble, and the residuals are calculated:

$$v_{\text{pec2},i} = v_{\text{LSR},i} - v_{\text{rad},i} - D_0 \cos(l_i - l_0) \cos b_i. \quad (8)$$

The ϵ_i are also estimates for the errors in the $v_{\text{pec2},i}$. Assume that the $v_{\text{pec2},i}$ are samples of a Gaussian random variable. Figure 2 compares the cumulative distribution of v_{pec2} for the data in Table 1 with Gaussian distributions having $\sigma = 7.8 \text{ km s}^{-1}$, $\sigma = 4.8 \text{ km s}^{-1}$, and $\sigma = 10.8 \text{ km s}^{-1}$. Given the number of times the data crosses the $\sigma = 7.8 \text{ km s}^{-1}$ curve, there is no reason to suspect that the values of v_{pec2} have a non-Gaussian distribution; the data are adequately represented by a Gaussian distribution, and the Gaussian random variable assumption is consistent. Also assume that the ϵ_i are true 1σ Gaussian errors in the $v_{\text{pec2},i}$ instead of just estimates—this is not true but should be a good approximation as long as ϵ_{max} is kept small. If there were no errors, the $v_{\text{pec2},i}$ would be perfectly

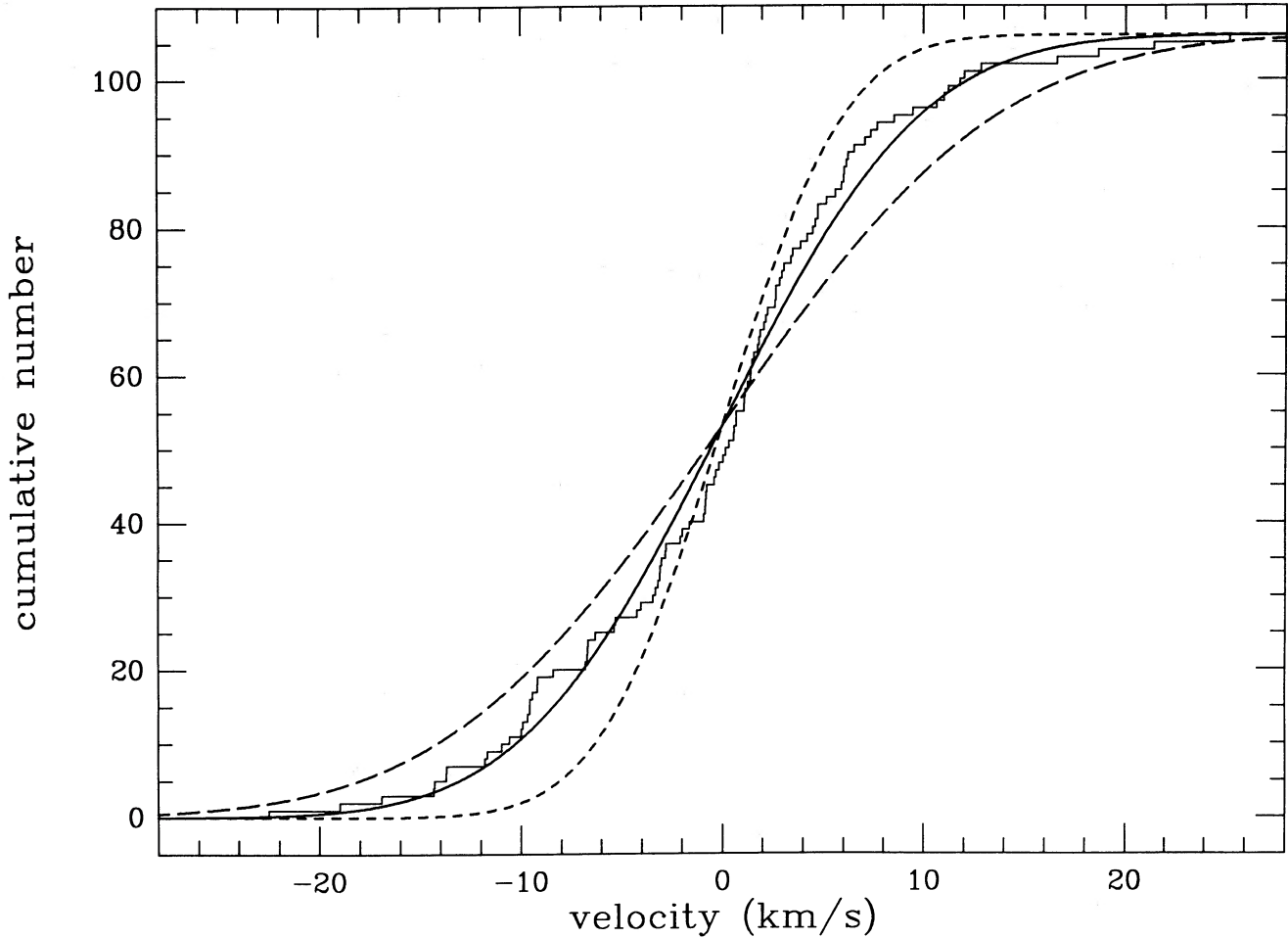


FIG. 2.—Cumulative distribution of the residual peculiar velocities $v_{\text{pec}2}$ from Table 1. The superposed curves are the expected distribution for Gaussian velocity dispersions with $\sigma_v = 7.8 \text{ km s}^{-1}$ (thin solid curve), $\sigma_v = 10.8 \text{ km s}^{-1}$ (dashed curve), and $\sigma_v = 4.8 \text{ km s}^{-1}$ (dotted curve).

known, and they would be samples of the molecular cloud velocity distribution function, with dispersion σ_v :

$$f(v, \sigma_v) = (2\pi\sigma_v^2)^{-1/2} \exp(-v^2/2\sigma_v^2). \quad (9)$$

Since the $v_{\text{pec}2,i}$ are not perfectly known, each is actually a sample of a slightly different distribution function:

$$f(v, \sigma_v, \epsilon_i) = [2\pi(\sigma_v^2 + \epsilon_i^2)]^{-1/2} \exp\left[-\frac{v^2}{2(\sigma_v^2 + \epsilon_i^2)}\right]. \quad (10)$$

For a given subset of the catalog, the *a posteriori* probability of having observed that collection of $v_{\text{pec}2,i}$ is given by the likelihood function

$$\mathcal{L}(\sigma_v, \epsilon_{\text{max}}) = \prod_{\epsilon_i < \epsilon_{\text{max}}} f(v_{\text{pec}2,i}, \sigma_v, \epsilon_i), \quad (11)$$

which can be normalized to unit probability:

$$\mathcal{L}_0(\sigma_v, \epsilon_{\text{max}}) \equiv \mathcal{L}(\sigma_v, \epsilon_{\text{max}}) \left[\int_0^\infty \mathcal{L}(\sigma_v, \epsilon_{\text{max}}) d\sigma_v \right]^{-1}. \quad (12)$$

The best estimate of σ_v is that value of σ_v for which \mathcal{L} is maximized. Figure 3 shows $\mathcal{L}_0(\sigma_v, 3.5 \text{ km s}^{-1})$. The high and low 90% confidence limits are indicated. Note that this function falls off very rapidly for small σ_v : the probability density at $\sigma_v = 4 \text{ km s}^{-1}$ is seven orders of magnitude smaller than the peak. That is, the probability of having observed this set of

data if the velocity dispersion were 4 km s^{-1} is $\sim 10^{-7}$ of the probability of having observed this set of data if the velocity dispersion were 7.8 km s^{-1} .

We cannot accept peculiar velocities with arbitrarily large errors. When $\epsilon_i \gtrsim \sigma_v$, the result becomes unreliable because the ϵ_i are not actually true 1σ errors. The error in the ϵ_i (the error in the estimated error) becomes confused with the dispersion, σ_v . Figure 4 indicates the behavior of the likelihood function \mathcal{L} as data are added—the most likely value of σ_v (peak) and the 90% confidence limits (high and low) are plotted as a function of ϵ_{max} . The function is generally well behaved, although the values of σ_v tend to drift upward for $\sigma_v \gtrsim \epsilon_{\text{max}}$. The value $\epsilon_{\text{max}} = 3.5 \text{ km s}^{-1}$ was chosen for the examples above because it has $\epsilon_{\text{max}} \approx 0.5\sigma_v$ and therefore yields reliable results. This subset (Table 1) of the catalog yields $\sigma_v = 7.8 \pm 0.6 \text{ km s}^{-1}$ (these are 1σ errors, the 68% confidence limits from the likelihood function).

The clouds in Table 1 probably have masses in the range $10^{4.5} - 10^{5.5} M_\odot$, typical of clouds associated with H II regions in the solar neighborhood (e.g., Stark and Blitz 1978), but this is not certain because they have only been observed at a few points.

The entire analysis described in this section can be repeated with various rotation curves. The present result does have a contribution to the velocity dispersion that comes from the rotation curve. This can be seen in Figure 5, where the values

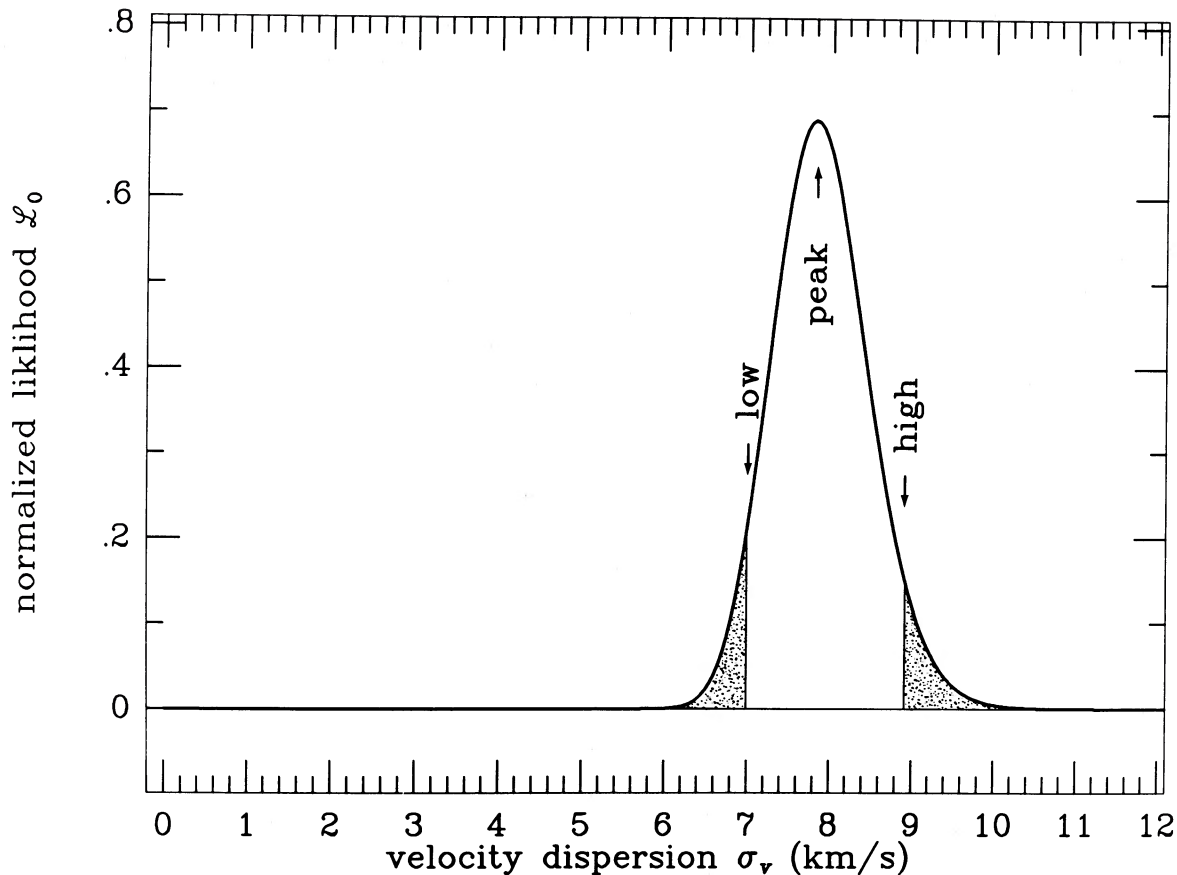


FIG. 3.—The normalized likelihood, \mathcal{L}_0 , that clouds listed in Table 1 are members of population with velocity dispersion σ_v . The shaded areas are each 5% of the total; the values of σ_v labeled “high” and “low” are the 90% confidence limits on the estimate indicated by “peak.”

of $v_{\text{pec}2}$ are displayed as the areas of a circle plotted at the appropriate position for the cloud in a map of the solar neighborhood. The sign of the $v_{\text{pec}2}$ tends to change from quadrant to quadrant: positive between $l = 0^\circ$ and $l = 90^\circ$; negative between $l = 90^\circ$ and $l = 180^\circ$; positive again between $l = 180^\circ$ and $l = 270^\circ$; negative again between $l = 270^\circ$ and $l = 360^\circ$. The magnitude of the effect is $\sim 3 \text{ km s}^{-1}(r/1 \text{ kpc}) \sin(2l)$. One way to think of this is an “error in the rotation curve,” where the adopted rotation curve (eq. [2]) is rising too fast through the solar neighborhood, so that we see the need for this “correction” to the Oort constant A . However, as Brand (1986) has shown, the rotation curve used is an excellent fit to additional data beyond the boundaries of Figure 5. The “correction” or “error in the rotation curve” is confined to the solar neighborhood. One manifestation of this discrepancy is the difference between local and global determinations of the Oort constant A . If a flatter rotation curve is used, the value of the dispersion found is somewhat smaller, $\sigma_v = 6.9 \text{ km s}^{-1}$. This is the main difference between the value of $\sigma_v = 7.8 \text{ km s}^{-1}$ found above, and the value $\sigma_v = 6.6 \text{ km s}^{-1}$ found in Paper I. This is not a significant change in the result.

On a given line of sight in the Milky Way, objects on circular orbits around the galactic center will occupy a particular range of velocities. Velocities not in this range are said to be “forbidden” to galactic rotation. In particular, positive velocities are forbidden in the second quadrant, and negative velo-

cities are forbidden in the third quadrant. A number of the clouds in Table 1 have forbidden velocities: S125, S220, S238, BFS48, BBW56, BBW240, BBW300B (19.3 km s^{-1}), and BBW309F. No change in the rotation curve can generate forbidden velocities. These velocities are so large that it strains credulity to explain them with a dispersion $\sigma_v \lesssim 5 \text{ km s}^{-1}$.

Another way to think of Figure 5 is a detection of “small-scale streaming” in the local GMCs (Brand 1986). It might be said, for example, that the negative velocities in the upper right of Figure 5 were the result of streaming in the Perseus arm. In other words, the peculiar velocities are correlated over a spiral arm feature and are therefore not truly random, and are not really “dispersion” but “small-scale streaming.” This is mostly a matter of definition, and in the definition of velocity dispersion adopted for this paper, the contribution from small-scale streaming should be included in the dispersion.

It may be that small-scale streaming motions originate by a different physical process than the truly random motions, and that it is useful to separate the two processes. This may be possible given a larger data set. It might then be possible to identify close pairs of clouds like S263 and S264, and BBW195A and BBW193B, which have very different velocities, even though they are in close proximity. These pairs would then be examples of random motions, and their velocity separations would give some measure of the random velocities. There is a large range in v_{pec} values toward $l \approx 270^\circ$. Some of

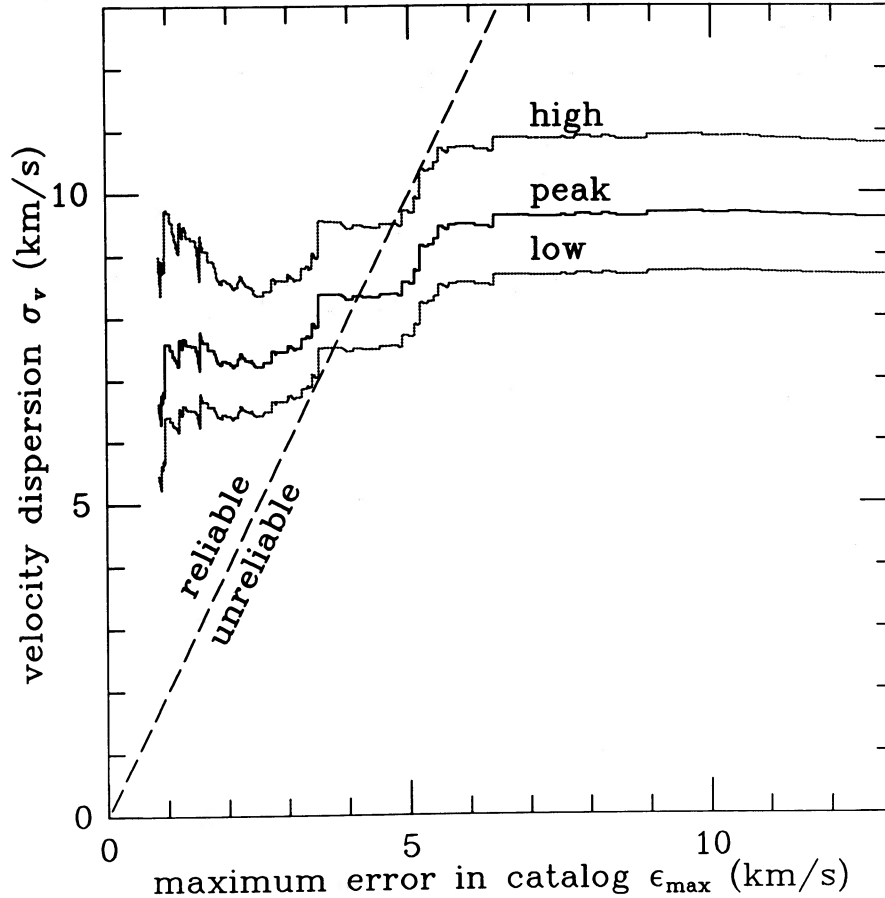


FIG. 4.—The behavior of the likelihood function with the addition of increasingly poor data. The curves labeled “high,” “low” and “peak” are the 90% confidence limits and the most likely value (see Fig. 3). These curves change discontinuously when a new cloud is added to the sample. If $\epsilon_{\max} \gtrsim \sigma_v$, systematic errors can cause the result to be unreliable.

these pairs have velocity separations greater than 10 km s^{-1} . Values less than 3 km s^{-1} for the velocity dispersion are therefore improbable, even if streaming motions are excluded.

III. DISCUSSION AND COMPARISON WITH OTHER WORK

The velocity dispersion of molecular clouds can be determined in other parts of the Galaxy and in other galaxies, using methods which are different from that of § II. These values tend to be comparable to or smaller than 7.8 km s^{-1} . The discussion in this section argues for the plausibility of this “large” result in light of the other measurements, by means of a critical comparison.

It should first be pointed out that comparisons between the velocity dispersion of nearby clouds and velocity dispersions in other parts of the Galaxy carry an implicit and possibly untrue assumption that the velocity dispersion is constant or slowly varying throughout the Galaxy, and that local GMCs are typical of the Galaxy as a whole. The velocity dispersion in the solar neighborhood can have one value, and the velocity dispersion in the molecular ring another. The Galactic center region is an extreme example: the cloud-cloud velocity dispersion there is 15 or 20 km s^{-1} (Bally *et al.* 1988). Molecular gas is usually gravitationally bound into clouds, but only weakly so, and is therefore affected by tidal shear, a force which varies greatly throughout the Galaxy. Jog and Ostriker (1988) have

considered a model in which cloud random velocities originate in the rotational energy of the galactic disk, and predict that σ_v should increase slightly with decreasing galactocentric distance.

There is a considerable amount of observational data on the molecular ring at 5 kpc, and various workers have tried different methods to obtain the dispersion from those data.

1. The roughness of the terminal velocity as a measure of dispersion. This method was used by Gordon and Burton (1976), and Liszt, Burton, and Xiang (1984). The terminal velocity $v(l)$ in the first quadrant of the Galaxy is found as a function of l , and the dispersion is the rms of the (positive) deviations from the tangent velocity: $\sigma_v = \langle [v_c - v(l)]^2 \rangle^{1/2}$. The difficulty with this method is the determination of $v(l)$. Either H I or CO data can be used to try to determine $v(l)$; the two show similar kinematics, since the molecular and atomic components of the interstellar medium are well mixed. Both CO and H I data show fluctuations in the terminal velocity on various scales and with amplitudes of many kilometers per second. If the curve $v(l)$ is allowed many degrees of freedom, then it will follow these fluctuations exactly, and the resulting “dispersion” will be small; if the curve is constrained to be smooth over large scales, then the dispersion is larger. It is an error to allow $v(l)$ so much freedom that it can take on independent values over scales smaller than the mean separation between cloud complexes; $v(l)$ should be stiff over scales of

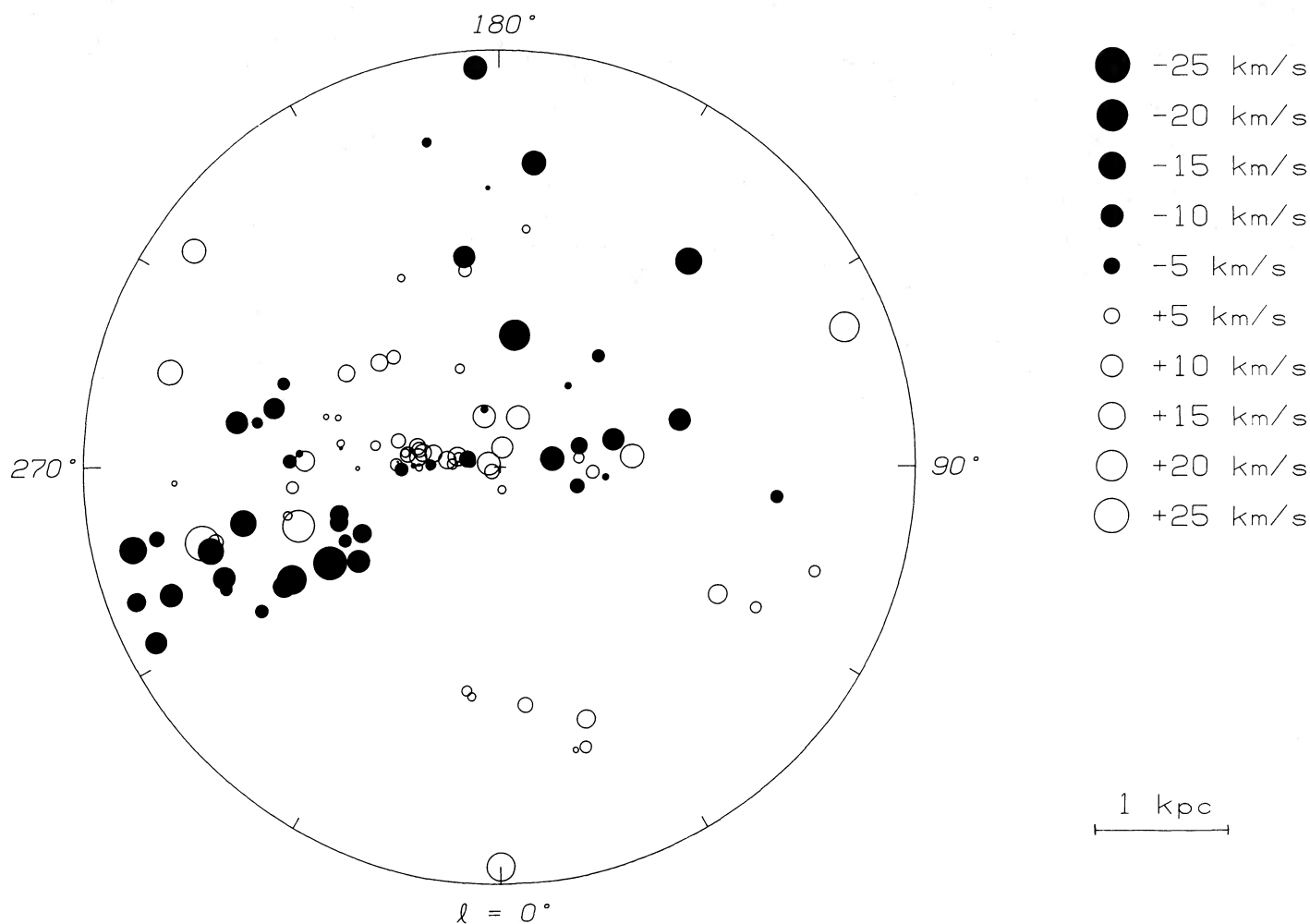


FIG. 5.—A representation of the residual peculiar velocities of nearby giant molecular clouds. The Earth is at the center of the figure, galactic longitudes are marked around the edge of the frame. The position of each GMC in Table 1 is marked by a circle whose area and shading represent the magnitude and sign of its residual peculiar velocity. The density of clouds is determined largely by selection effects.

~200 pc. No one analyzing first quadrant CO data has yet done this properly.

2. The width of the tangent velocity feature in composite spectra, used by Knapp, Stark, and Wilson (1985) and Clemens (1985). Suppose the CO distribution in the Galaxy were very fine grained, so that any telescope beam in the galactic plane would see many clouds. In the absence of velocity dispersion, the tangent velocity crowding would result in infinitely higher density at the tangent point than at other velocities. A galactic survey spectrum would be a δ -function at the tangent velocity. With some added dispersion, the infinite peak smears out into a Gaussian whose width is the dispersion. The idea behind this method is that the CO distribution may appear fine grained when viewed with a sufficiently large beam, and that large beams can be synthesized by averaging small beams together. The problem is that the fine grained assumption breaks down because the molecular cloud distribution is very lumpy and correlated over scales of tens to hundreds of parsecs, and this lumpiness causes systematic underestimation of the velocity dispersion. The molecular cloud velocity dispersion values derived by Clemens (1985) suffer from this problem: the composite spectrum is obtained from a region so small that only one GMC complex appears in the spectrum; Clemens' disper-

sions are actually *internal* dispersions of single molecular cloud complexes. Compare, for example, Clemens' description of the method used to obtain the value for the dispersion at $l = 31^{\circ}.5$, in Figure 1 of Clemens (1985), with the picture of this region in Knapp, Stark, and Wilson (1985, p. 274). A number of composite spectra made with a synthesized beam are shown in Figure 3 of Knapp, Stark, and Wilson (1985). Many of these have a "last feature" at the terminal velocity which contains several GMC complexes, and which has a width corresponding to a cloud-cloud velocity dispersion of $\sim 7 \text{ km s}^{-1}$.

3. The scale height of molecular clouds is a measure of velocity dispersion, given the reasonable assumptions that the lifetime of the cloud is long compared to the oscillation period in the \hat{z} -direction and that the cloud motions are largely ballistic (e.g., Stark and Blitz 1978). The \hat{z} -velocity dispersion need not have the same value as the dispersion in directions lying in the plane although the velocity ellipsoid for extreme Population I objects tends to be spherical. To convert the scale height into a velocity dispersion requires the mass distribution in the Galaxy—this can be estimated with reasonable accuracy (Caldwell and Ostriker 1981). The scale height for small- and medium-size clouds is larger than that of very large clouds (Stark 1979, 1983; Scoville *et al.* 1987). The estimated values for

the velocity dispersion of clouds up to $\sim 2 \times 10^5 M_\odot$ is $\sim 8 \text{ km s}^{-1}$, while the dispersion of very massive GMCs is less, $\sim 3 \text{ km s}^{-1}$. This may be a partial explanation of the small ($\approx 3 \text{ km s}^{-1}$) values found by Liszt, Burton, and Xiang (1984): by measuring the dispersion at the tangent velocities at $b = 0^\circ$, they are selectively observing a population of extremely massive cloud complexes having a lower velocity dispersion. In the solar neighborhood, Dame *et al.* (1987) find a scale height of 87 pc HWHM, which implies $\sigma_v \approx 8 \text{ km s}^{-1}$ (Knapp 1987).

In other galaxies, beams of millimeter telescopes usually include many molecular clouds. In that case, the observed line width is at least as large as the velocity distribution function (eq. [9]). Almost all normal spiral galaxies have line widths larger than 25 km s^{-1} ; the narrowest line in a normal spiral is NGC 5434, at 20 km s^{-1} . This is compatible with most spirals having $\sigma_v \gtrsim 8 \text{ km s}^{-1}$.

A correct calculation of the velocity dispersion requires a sufficiently large sample of clouds to populate the velocity distribution and an accurate knowledge of the mean orbital velocity at the position of each cloud. Spuriously low values can be

obtained if these conditions are not met. Clemens (1985) restricted the sampled volume until it contained too few clouds. Liszt, Burton, and Xiang (1984) used gas associated with the molecular clouds themselves to determine the rotation velocity. This explains the discrepancies with the result obtained in § II.

IV. CONCLUSIONS

1. Our conclusions can be summed up as follows. The one-dimensional rms radial velocity dispersion of GMCs in the solar vicinity ($r < 3 \text{ kpc}$) is $\sigma_v = 7.8^{+0.6}_{-0.5}$. This quantity includes a non-random component (i.e., small-scale streaming). Note that this sample does not include many extremely massive GMCs ($> 10^6 M_\odot$).

2. The molecular material in the solar neighborhood seems to have a net drift of $3.8 \pm 0.9 \text{ km s}^{-1}$ toward $l = 292^\circ \pm 16^\circ$ with respect to the LSR.

We thank D. Clemens, M. Fich, and G. R. Knapp for discussions.

REFERENCES

- Bally, J., Stark, A. A., Wilson, R. W., and Henkel, C. 1988, *Ap. J.*, **324**, 223.
 Blitz, L., Fich, M., and Stark, A. A. 1982, *Ap. J. Suppl.*, **49**, 183 (BFS).
 Brand, J. 1986, Ph.D. thesis, Leiden University.
 Brand, J., Blitz, L., and Wouterloot, J. G. A. 1986, *Astr. Ap. Suppl.*, **65**, 537 (BBW).
 Brand, J., Blitz, L., Wouterloot, J. G. A., and Kerr, F. J. 1987, *Astr. Ap. Suppl., Ser* **68**, 1: **69**, 343.
 Caldwell, J. A. R., and Ostriker, J. P. 1981, *Ap. J.*, **251**, 61.
 Chini, R., and Wink, J. E. 1984, *Astr. Ap.*, **139**, L5.
 Clemens, D. P. 1985, *Ap. J.*, **295**, 422.
 Dame, T. M., *et al.* 1987, *Ap. J.*, **322**, 706.
 Delhaye, J. 1965, in *Galactic Structure*, ed. A. Blaauw and M. Schmidt (Chicago: University of Chicago Press), p. 72.
 Forbes, D. 1984, *A.J.*, **89**, 475.
 Gordon, M. A., and Burton, W. B. 1976, *Ap. J.*, **208**, 346.
 Jog, C. J., and Ostriker, J. P. 1988, *Ap. J.*, **328**, 404.
 Knapp, G. R. 1987, *Pub. A.S.P.*, **99**, 1134.
 Knapp, G. R., Stark, A. A., and Wilson, R. W. 1985, *A.J.*, **90**, 254.
 Liszt, H. S., Burton, W. B., and Xiang, D.-L. 1984, *Astr. Ap.*, **140**, 303.
 Scoville, N. Z., Yun, M. S., Clemens, D. P., Sanders, D. B., and Waller, W. H. 1987, *Ap. J. Suppl.*, **63**, 821.
 Stark, A. A. 1979, Ph.D. thesis, Princeton University.
 ———. 1983, in *Kinematics, Dynamics, and Structure of the Milky Way*, ed. W. L. H. Shuter (Dordrecht: Reidel), p. 127.
 ———. 1984, *Ap. J.*, **281**, 624 (Paper I).
 Stark, A. A., and Blitz, L. 1978, *Ap. J. (Letters)*, **225**, L15.

JAN BRAND: Osservatorio Astrofisico di Arcetri, Largo Enrico Fermi 5, 50125 Firenze, Italy

ANTONY A. STARK: HOH L-231, Crawford Hill, AT&T Bell Laboratories, Holmdel, NJ 07733-1988